ARTICLE

Linear Tricationic Room-Temperature Ionic Liquids: Synthesis, Physiochemical Properties, and Electrowetting Properties

Eranda Wanigasekara,[†] Xiaotong Zhang,[†] Yasith Nanayakkara,[†] Tharanga Payagala,[†] Hyejin Moon,[‡] and Daniel W. Armstrong*[,†]

Department of Chemistry and Biochemistry and Department of Mechanical and Aerospace Engineering, The University of Texas at Arlington, Arlington, Texas 76019-0065

ABSTRACT Efficient and facile synthesis of novel linear tricationic room-temperature ionic liquids was performed, and their physiochemical properties were determined. Different physiochemical properties were observed according to the structural variations such as the cationic moiety and the counteranion of the ionic liquid. The electrowetting properties of these ionic liquids were also investigated, and linear tricationic ionic liquids were shown to be advantageous as effective electrowetting materials due to their high structural flexibility.

KEYWORDS: room-temperature ionic liquid • electrowetting

1. INTRODUCTION

Room-temperature ionic liquids (RTILs) are a class of salts that are liquids at or near room temperature (1). Recently RTILs have attracted much attention in academic research and industry, since they have shown profound advantages in the context of green chemistry and have great technological potential (2−4). Recently monocationic, dicationic, and tricationic ionic liquids have been used extensively in the field of analytical chemistry as ion-pairing reagents for the ultra trace detection of anions in the positive mode of electrospray ionization mass spectrometry (ESI-MS) (5), high thermal stability gas chromatographic (GC) stationary phases (6), capillary electrophoresis (CE) (7), and electrowetting applications (8). We have recently reported the synthesis and physiochemical properties of a series of dicationic and tricationic ionic liquids (9). These reported ILs possessed good thermal stabilities and higher viscosities in comparison to monocationic ILs (10). Moreover, it was shown by Payagala et al. that physicochemical properties such as viscosity, density, thermal stability, melting point, and solubility behaviors can be varied (tuned) to a greater extent in multicationic ILs than in the conventional ILs by changing the cation type, linkage chain length, etc. (9). However, the tuning capability for trigonal tricationic ILs (9b) was lower than that of linear dicationic ILs (9a). This was because, in most of the trigonal ILs synthesized, there were only two methylene moieties between the rigid trigonal core and the three pendant cationic moieties. The rigid trigonal geometry and the existence of three charge-carrying moieties in close proximity resulted in high apparent polarity and relatively high melting salts. On the basis of these observations, it was concluded that, for multicationic ILs, the linear geometry would give the best tunability in terms of physicochemical properties and the highest probability of forming RTILs.

The interesting physicochemical properties of the ILs have led to their use in applications involving electrowetting on dielectric-based microfluidic devices (8). Electrowetting (EW) is the decrease in contact angle when an external voltage is applied across the solid/liquid interface. Simple EW which utilizes a metal base to hold the droplet is often associated with the drawback of droplet instability with change of the voltage, whereas electrowetting on a dielectric solid (e.g., Teflon) produces stable and reversible droplet shape with changes in the voltage (18). Since reversibility of the droplet shape with a change in voltage is an important factor in microfluidic devices, electrowetting on dielectric (EWOD) has shown greater success in applications such as fluid lens systems, electrowetting displays, optical filters, paint drying, micromotors, electronic microreactors, and controlling fluids in multichannel structures (18−22). Water or aqueous electrolytes are used in nearly all EWOD devices. Water-based systems are known to create complications due to their evaporation, low thermal stability, and tendency to contribute to corrosion in integrated electronics (18). The unique properties of RTILs, including negligible vapor pressure, ultra high stability over a wide temperature range, and large electrochemical windows, (1) make them ideal in EWOD applications over traditional aqueous or electrolyte solutions. Recently a detailed study was carried out to find the electrowetting properties of traditional and multifunctional ILs (8). These EWOD-based micro reactors and micro extraction devices have been used in various scientific areas. Dubois et al. demonstrated the use of IL droplets as electronic microreactors on open digital microfluidic chips (24).

[†] Department of Chemistry and Biochemistry.

[‡] Department of Mechanical and Aerospace Engineering.

Received for review January 20, 2009 and accepted August 29, 2009

DOI: 10.1021/am900519j

Published on Web 09/22/2009

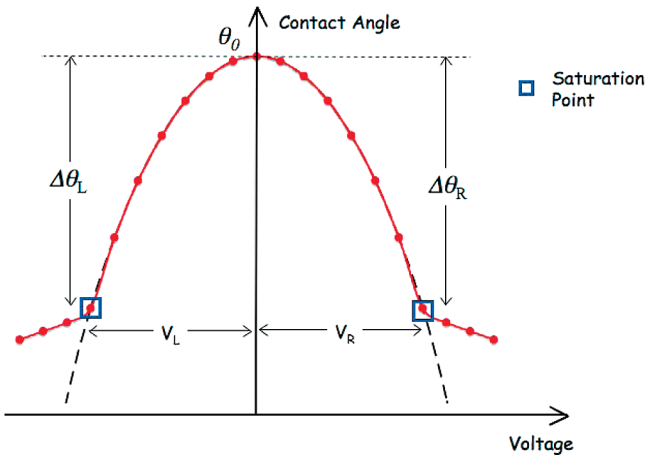

FIGURE 1. Plot of contact angle vs voltage according to Young's and Lippmann's equation.

Also, Chatterjee et al. recently demonstrated that ILs can be used in digital microfluidic devices (25). Moon et al. used ILs in an EWOD-based micro heat transfer device, and Kunchala et al. used an IL in a EWOD-based liquid−liquid extraction device (26).

The contact angle θ between a dielectric surface and an ionic liquid droplet under an external voltage of V is derived from a combination of Young's and Lippmann's equations (eq 1) (8a, 8b).

$$\cos\theta = \cos\theta_0 + \frac{c}{2\gamma}V^2 = \cos\theta_0 + \frac{\varepsilon\varepsilon_0}{2\gamma t}V^2 \qquad (1)$$

Here, c is the capacitance per unit area (specific capacitance), ε is the relative permittivity of the dielectric layer (dielectric constant), ε_0 is the permittivity of a vacuum, γ is the surface tension of the liquid, t is the thickness of the dielectric layer, θ is the contact angle at the designated voltage across a dielectric layer, and θ_0 is the contact angle at zero voltage. As the voltage increases, the contact angle also increases according to eq 1. After a certain point, the contact angle starts to deviate from regular behavior with increasing voltage. The voltage and corresponding contact angle where this occurs is referred to as the saturation voltage and saturation angle, respectively. According to eq 1, a plot of contact angle versus applied voltage should give a parabolic graph, as shown in Figure 1.

Our previous studies have shown the use of a series of RTILs in EW experiments and a correlation between contact angle variation and the structure of the ionic liquid (IL). Monocationic, dicationic, and tricationic ILs were used in those experiments. The trigonal tricationic ILs in our previous study were of trigonal geometry and, hence, had a relatively rigid structure (9b).

In this study, we report the synthesis and physiochemical properties and electrowetting properties of linear tricationic ionic liquids (LTILs) for the first time. Furthermore, we explore the electrowetting properties and their correlation with structural flexibility.

2. EXPERIMENTAL SECTION

The structures of the LTILs synthesized are illustrated in Figure 2, and Scheme 1 illustrates the synthesis of the core structure.

2.1. Materials. The reagents required for synthesis included anhydrous dimethylformamide, anhydrous acetonitrile, anhydrous tetrahydrofuran, sodium imidazole, 1,3-dibromopropane, 1,6-dibromohexane, 1,10-dibromodecane, methylimidazole, butylimidazole, benzylimidazole, and tripropylphosphine, which were purchased from Sigma-Aldrich (Milwaukee, WI). All chemicals were of reagent grade and were used without further purification. For column chromatography, silica gel 60 Å (Sorbent Technologies, Inc.; 200−425 mesh) was used.

2.2. Procedure for the Synthesis of the Core Structure 1-(Bromodecyl)-3-(bromodecyl)imidazolium Bromide Salt (1a). Sodium imidazole (1.0 g, 12.1 mmol) in 20 mL of anhydrous DMF was added slowly to a solution of dibromodecane (18.2 g, 60.5 mmol) in 100 mL of anhydrous DMF by using a syringe pump over a period of 3 h at room temperature. After completion of the addition, the reaction mixture was heated to 70 °C for 12 h. Then DMF was evaporated under vacuum and the resulting crude material was washed with hexane (5 × 100 mL) to remove excess dibromoalkane. At this point the resulting crude product was subjected to column chromatography using CH_3OH/CH_2Cl_2 (1:9) as the eluent system. The purified product was then dried under vacuum overnight to give the desired product in 65% yield. ^{1}H NMR (300 MHz, DMSO-d_6): δ 9.21 (s, 1H), 7.80 (d, J = 1.7 Hz, 2H), 4.15 (t, J = 7 Hz, 4H), 3.51 (t, J = 7 Hz, 4H), 1.77 (m, 8H), 1.33 (m, 4H), 1.24 (br s, 20H). ^{13}C NMR (75 MHz, DMSO-d_6): δ 136.4, 123.02, 49.4, 35.8, 32.7, 29.7, 29.2, 28.8, 28.6, 28.0, 25.9. Anal. Calcd for $C_{23}H_{43}N_2$: C, 47.04; H, 7.38; Br, 40.82; N, 4.77. Found: C, 47.08; H, 7.42; N, 4.81. ESI-MS (m/z): calcd 507.41 (M^+), found 507.25.

2.3. Procedure for the Synthesis of the Core Structure 1-(Bromohexyl)-3-(bromohexyl)imidazolium Bromide Salt (1b). This compound was prepared by a procedure similar to that described above for **1a**. Sodium imidazole (1.0 g, 12.1 mmol) in 20 mL of anhydrous DMF was added slowly to a solution of dibromodecane (14.8 g, 60.5 mmol) in 100 mL of anhydrous DMF by using a syringe pump over a period of 3 h at room temperature. After completion of the addition, the solution was stirred for an additional 12 h. Then DMF was evaporated under vacuum and the resulting crude material was washed with hexane (5 × 100 mL) to remove excess dibromoalkane. At this point the resulting crude product was subjected to column chromatography using CH_3OH/CH_2Cl_2 (1:9) as the eluent system. The purified product was then dried under vacuum overnight to give the desired product in 72% yield. ^{1}H NMR (300 MHz, DMSO-d_6): δ 9.38 (s, 1H), 7.84 (s, 2H), 4.18−4.13 (t, J = 7.2 Hz, 4H), 3.50−3.46 (t, J = 6.5 Hz, 4H), 1.81−1.70 (m, 8H), 1.41−1.31 (m, 4H), 1.25−1.15 (m, 4H). ^{13}C NMR (75 MHz, DMSO-d_6): δ 136.48, 122.94, 60.93, 49.29, 32.69, 29.87, 25.86, 25.34. Anal. Calcd for $C_{15}H_{27}N_2$: C, 37.92; H, 5.73; N, 5.90. Found: C, 37.93; H, 5.80; N, 5.95. ESI-MS (m/z): calcd 475.10 (M^+), found 475.10.

2.4. Procedure for the Synthesis of the Core Structure 1-(Bromopropyl)-3-(bromopropyl)imidazolium Bromide Salt (1c). This compound was prepared by a procedure similar to that for **1b**. ^{1}H NMR (300 MHz, DMSO-d_6): δ 9.27 (s, 1H), 7.83 (d, J = 1.4 Hz, 2H), 4.28 (t, J = 7 Hz, 4H), 3.54 (t, J = 7 Hz, 4H), 2.37 (m, 4H). ^{13}C NMR (75 MHz, DMSO-d_6): δ 136.4, 122.9, 49.3, 29.9, 29.2, 28.9, 20.4, 19.8, 15.9, 15.2. Anal. Calcd for $C_9H_{15}N_2$: C, 27.65; H, 3.87; Br, 61.32; N, 7.17. Found: C, 27.68; H, 3.92; N, 7.20. ESI-MS (m/z): calcd 311.04 (M^+), found 311.00.

2.5. Procedure for the Synthesis of LTILs 2a−d, 3a−d, and 4a−d. All the reactions were carried out in tetrahydrofuran (THF), except for **4a−d**, for which acetonitrile (ACN) was used as the reaction solvent. The linear core structures **1a−c** (1 equiv in THF or ACN) were reacted with 2.5 equiv of methylimidazole,

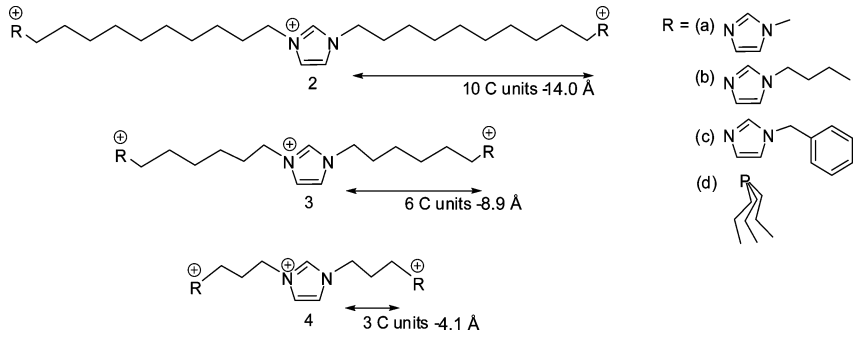

FIGURE 2. Structures of linear tricationic ionic liquids.

Scheme 1. Synthesis of LTIL with R-Substituted Imidazole as the Charge-Carrying Moiety

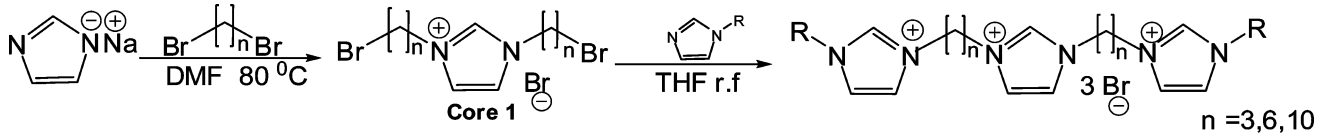

butylimidazole, benzylimidazole or tripropylphosphine under reflux over 36−48 h (phosphonium ILs need to be reacted for 48 h). Then the solvent was removed in vacuo and the resulting thick liquid or solid was dissolved in 5−10 mL of deionized water. The aqueous layer was then washed with ethyl acetate (6 × 100 mL), and water was removed in vacuo. The final product as the bromide salt was then dried under high vacuum (75−85% yield).

Final products were synthesized through a metathesis reaction of the bromide salts with lithium trifluoromethanesulfonimide ($LiNTf_2$), sodium tetrafluoroborate ($NaBF_4$), and lithium trifluoromethanesulfonate (LiTfO) according to the previously published procedure (9a).

2.5.1. ***1-(1′-Methyl-3′-decylimidazolium)-3-(1″-methyl-3″-decylimidazolium)imidazolium Tris[bis((trifluoromethyl)sulfonyl)imide] (2a).*** ^{1}H NMR (300 MHz, DMSO-d_6): δ 9.15 (s, 1 H), 9.08 (s, 2 H), 7.78 (d, J = 1.4 Hz, 2 H), 7.75 (t, J = 1.4 Hz, 2 H), 7.69 (t, J = 1.4 Hz, 2 H), 4.14 (t, J = 7.2 Hz, 8 H), 3.84 (s, 6 H), 1.65−1.80 (m, 8 H), 1.24 (br s, 26 H). ^{13}C NMR (75 MHz, DMSO-d_6): δ 137.2, 136.4, 124.1, 122.9, 122.8, 49.3, 49.2, 36.3, 29.9, 29.3, 28.9, 26.06. ^{19}F NMR (282 MHz): δ −78.6. Anal. Calcd for $C_{37}H_{55}N_9$: C, 32.86; H, 4.10; N, 9.32. Found: C, 32.89; H, 4.15; N, 9.38. ESI-MS (m/z): calcd 170.48 (M^{3+}), found 170.50.

2.5.2. ***1-(1′-Butyl-3′-decylimidazolium)-3-(1″-butyl-3″-decylimidazolium)imidazolium Tris[bis((trifluoromethyl)sulfonyl)imide] (2b).*** ^{1}H NMR (300 MHz, DMSO-d_6): δ 9.17 (s, 1 H), 9.15 (s, 2 H), 7.80−7.77 (m, 6 H), 4.18−4.11 (q, J = 6.8 Hz, 12 H), 1.81−1.74 (m, 12H), 1.30−1.18 (br s, 28 H), 0.89 (t, J = 7.5 Hz, 6H). ^{13}C NMR (75 MHz, DMSO-d_6): δ 136.5, 122.9, 122.8, 49.3, 49.0, 31.8, 29.8, 29.2, 28.8, 26.0, 19.3, 13.8. ^{19}F NMR (282 MHz): δ −78.6. Anal. Calcd for $C_{43}H_{67}N_9$: C, 35.95; H, 4.70; N, 8.78. Found: C, 35.50; H, 4.65; N, 8.80. ESI-MS (m/z): calcd 198.51 (M^{3+}), found 198.58.

2.5.3. ***1-(1′-Benzyl-3′-decylimidazolium)-3-(1″-benzyl-3″-decylimidazolium)imidazolium Tris[bis((trifluoromethyl)sulfonyl)imide] (2c).*** ^{1}H NMR (300 MHz, DMSO-d_6): δ 9.25 (s, 2 H), 9.12 (s, 1 H), 7.79−7.75 (m, 6 H), 7.38 (d, J = 1.7 Hz, 10 H), 5.38 (s, 2 H), 4.14 (q, J = 7 Hz, 8H), 1.79−1.72 (m, 8 H), 1.20 (br s, 24 H). ^{13}C NMR (75 MHz, DMSO-d_6): δ 136.6, 136.4, 135.4, 129.5, 129.3, 128.7, 123.3, 123.1, 122.9, 52.4, 49.5, 29.8, 29.3, 28.8, 26.1. ^{19}F NMR (282 MHz): δ −78.6. Anal. Calcd for $C_{49}H_{63}N_9$: C, 39.12; H, 4.22; N, 8.38. Found: C, 39.18; H, 4.26; N, 8.42. ESI-MS (m/z): calcd 221.17 (M^{3+}), found 221.25.

2.5.4. ***1-(Decyltripropylphosphonium)-3-(decyltripropylphosphonium)imidazolium Tris[bis((trifluoromethyl)sulfonyl)imide] (2d).*** ^{1}H NMR (300 MHz, DMSO-d_6): δ 9.33 (s, 1 H), 7.83 (d, J = 1.4 Hz, 2 H), 4.18 (t, J = 7.2 Hz, 4 H), 2.17−2.10 (m, 18 H), 1.77−1.73 (m, 18 H), 1.37−1.22 (m, 20 H), 0.98 (t, J = 7 Hz, 18 H). ^{13}C NMR (75 MHz, DMSO-d_6): δ 136.4, 122.9, 49.3, 29.9, 29.3, 28.8, 26.1, 21.24, 20.4, 19.8, 18.5, 17.9, 15.9, 15.2. ^{19}F NMR (282 MHz): δ −78.6. Anal. Calcd for $C_{47}H_{85}N_5$: C, 37.42; H, 5.68; N, 4.64. Found: C, 37.75; H, 5.70; N, 4.68. ESI-MS (m/z): calcd 222.54 (M^{3+}), found 222.56.

2.5.5. ***1-(1′-Methyl-3′-hexylimidazolium)-3-(1″-methyl-3″-hexylimidazolium)imidazolium Tris[bis((trifluoromethyl)sulfonyl)imide] (3a).*** ^{1}H NMR (300 MHz, DMSO-d_6): δ 9.50 (s, 1H), 9.35 (s, 2 H), 7.86 (s, 2 H), 7.84 (s, 2 H), 7.73 (s, 2 H), 4.17 (m, 8 H), 3.84 (s, 6 H), 1.77 (m, 8 H), 1.24 (m, 8H). ^{13}C NMR (75 MHz, DMSO-d_6): δ 137.07, 136.57, 124.09, 122.96, 122.82, 49.15, 49.08, 36.35, 29.63, 29.56, 25.32. ^{19}F NMR (282 MHz): δ −78.6. Anal. Calcd for $C_{29}H_{39}N_9$: C, 28.09; H, 3.17; N, 10.17. Found: C, 28.11; H, 3.20; N, 10.20. ESI-MS (m/z): calcd 133.10 (M^{3+}), found 133.10.

2.5.6. ***1-(1′-Butyl-3′-hexylimidazolium)-3-(1″-butyl-3″-hexylimidazolium)imidazolium Tris[bis((trifluoromethyl)sulfonyl)imide (3b).*** ^{1}H NMR (300 MHz, DMSO-d_6): δ 9.47 (s, 1H), 9.43 (s, 2 H), 7.86 (s, 4 H), 7.84 (s, 2H), 4.17 (t, J = 7.2 Hz, 12 H), 1.79−1.72 (m, 12 H), 1.24−1.17 (m, 12H), 0.85 (t, J = 7.2 Hz, 6H). ^{13}C NMR (75 MHz, DMSO-d_6): δ 136.56, 122.94, 49.17, 49.07, 31.84, 29.57, 25.32, 19.32, 13.84. ^{19}F NMR (282 MHz): δ −78.6. Anal. Calcd for $C_{35}H_{51}N_9$: C, 31.75; H, 3.88; N, 9.52. Found: C, 31.78; H, 3.90; N, 9.55. ESI-MS (m/z): calcd 161.14 (M^{3+}), found 161.10.

2.5.6. ***1-(1′-Benzyl-3′-hexylimidazolium)-3-(1″-methyl-3″-hexylimidazolium)imidazolium Tris[bis((trifluoromethyl)sulfonyl)imide] (3c).*** ^{1}H NMR (300 MHz, DMSO-d_6): δ 9.52 (s, 1H), 9.44 (s, 2 H), 7.85 (s, 6 H), 7.44−7.34 (m, 10 H), 5.45 (s, 4 H), 4.19−4.15 (m, 8 H), 1.77 (s, 8 H), 1.24 (m, 8H). ^{13}C NMR (75 MHz, DMSO-d_6): δ 136.68, 135.49, 129.53, 129.43, 128.86, 123.37, 123.05, 122.98, 52.34, 49.31, 49.17, 29.60, 29.53, 25.35. ^{19}F NMR (282 MHz): δ −78.6. Anal. Calcd for $C_{41}H_{47}N_9$: C, 35.37; H, 3.40; N, 9.05. Found: C, 35.39; H, 3.45; N, 9.10. ESI-MS (m/z): calcd 183.79 (M^{3+}), found 183.85.

2.5.7. ***1-(Hexyltripropylphosphonium)-3-(hexyltripropylphosphonium)imidazolium Tris[bis((trifluoromethyl)sulfonyl)imide] (3d).*** ^{1}H NMR (300 MHz, DMSO-d_6): δ 9.55 (s, 1H), 7.87 (s, 2 H), 4.21 (t, J = 6.9 Hz, 4 H), 2.24−2.12 (m, 16 H), 1.85−1.75 (m, 4 H), 1.56−1.26 (m, 24 H) 1.00−0.95 (t, J = 6.8 Hz, 18H). ^{13}C NMR (75 MHz, DMSO-d_6): δ 136.62, 122.98, 49.22, 29.55, 25.32, 21.09, 20.53, 19.91, 15.96, 15.74, 15.34. ^{19}F NMR (282 MHz): δ −78.6. Anal. Calcd for $C_{39}H_{69}N_5$: C, 33.55; H, 4.98; N, 5.02. Found: C, 33.60; H, 5.00; N, 5.05. ESI-MS (m/z): calcd 185.16 (M^{3+}), found 185.25.

2.5.8. ***(1′-Methyl-3′-propylmidazolium)-3-(1″-methyl-3″-propylimidazolium)imidazolium Tris[bis((trifluoromethyl)sulfonyl)imide]* (4a).** ^{1}H NMR (300 MHz, DMSO-d_6): δ 9.50 (s, 1 H), 9.32 (s, 2 H), 4.31−4.25 (m, 8 H), 3.87 (s, 6 H), 2.46−2.42 (m, 4 H). ^{13}C NMR (75 MHz, DMSO-d_6): δ 137.1, 123.0, 49.6, 26.0, 22.1, 20.4, 19.8, 15.9, 15.7, 15.3. ^{19}F NMR (282 MHz): δ −78.6. Anal. Calcd for $C_{23}H_{27}N_9$: C, 23.90; H, 2.35; N, 10.91. Found: C, 23.92; H, 2.40; N, 10.97. ESI-MS (*m*/*z*): calcd 105.07 (M^{3+}), found 105.17.

2.5.9. ***1-(1′-Butyl-3′-propylmidazolium)-3-(1″-butyl-3″-propylimidazolium)imidazolium Tris[bis((trifluoromethyl)sulfonyl)imide]* (4b).** ^{1}H NMR (300 MHz, DMSO-d_6): δ 9.50 (s, 1H), 9.43 (s, 2H), 7.90−7.84 (m, 6H), 4.32−4.29 (m, 8H), 4.19 (t, J = 7.2 Hz, 4H), 2.48−2.43 (m, 4H), 1.81−1.76 (m, 4H), 1.31−1.23 (m, 4H), 0.90 (t, J = 7.2, 6H). ^{13}C NMR (75 MHz, DMSO-d_6): δ 137.1, 136.8, 49.2, 46.4, 31.7, 29.9, 19.3, 13.8. ^{19}F NMR (282 MHz): δ −78.6. Anal. Calcd for $C_{29}H_{39}N_9$: C, 28.09; H, 3.17; F, 27.58; N, 10.17. Found: C, 28.09; H, 3.22; N, 10.20. ESI-MS (*m*/*z*): calcd 133.19 (M^{3+}), found 133.17.

2.5.10. ***1-(1′-Benzyl-3′-propylmidazolium)-3-(1″-benzyl-3″-propylimidazolium)imidazolium Tris[bis((trifluoromethyl)sulfonyl)imide]* (4c).** ^{1}H NMR (300 MHz, DMSO-d_6): δ 9.52 (s, 2 H), 9.48 (s, 1 H), 7.48−7.38 (m, 10 H), 5.47 (s, 4 H), 4.29 (q, J = 5.8 Hz, 8 H), 2.45 (m, 4 H). ^{13}C NMR (75 MHz, DMSO-d_6): δ 137.2, 123.0, 62.5, 49.4, 26.0, 22.1, 20.5, 19.9, 16.1, 15.9, 15.3. ^{19}F NMR (282 MHz): δ −78.6. Anal. Calcd for $C_{35}H_{35}N_9$: C, 32.14; H, 2.70; N, 9.64. Found: C, 32.14; H, 2.78; N, 9.65. ESI-MS (*m*/*z*): calcd 155.76 (M^{3+}), found 155.75.

2.5.11. ***1-(Propyltripropylphosphonium)-3-(propyltripropylphosphonium)imidazolium Tris[bis((trifluoromethyl)sulfonyl)imide]* (4d).** ^{1}H NMR (300 MHz, DMSO-d_6): δ 9.12 (s, 1 H), 7.84 (s, 2 H), 4.24 (t, J = 6.8, 4 H), 2.23−2.21 (m, 20 H), 0.57−1.47 (m, 12 H), 1.04−1.00 (m, 12 H), 1.04 (t, J = 7.2 Hz, 18 H). ^{13}C NMR (75 MHz, DMSO-d_6): δ 137.9, 123.0, 62.5, 49.6, 26.0, 22.1, 20.4, 19.8, 15.9, 15.3. ^{19}F NMR (282 MHz): δ −78.6. Anal. Calcd for $C_{33}H_{57}N_5$: C, 30.21; H, 4.38; N, 5.34. Found: C, 30.22; H, 4.44; N, 5.34. ESI-MS (*m*/*z*): calcd 157.13 (M^{3+}), found 155.17.

2.6. Glass Transition Temperature/Melting Point. The thermal measurements were performed with a differential scanning calorimeter (DSC, PerkinElmer Diamond DSC, 710 Bridgeport Ave., Shelton, CT). The Diamond DSC was calibrated using an indium primary standard, with solid−solid transitions for cyclohexane and ethylbenzene as supplementary low-temperature standards. IL samples (5−10 mg) were sealed in aluminum pans, and an empty aluminum pan was used as reference. The measurements were carried out in the temperature range of −120 °C to a predetermined temperature. The samples were sealed in aluminum pans and then heated and cooled at a scan rate of 10 °C min^{-1} under a flow of nitrogen. For solid compounds, the melting points were verified using a Mel-Temp capillary melting point apparatus (Cambridge, MA).

2.7. Density. The densities of the ionic liquids were determined at 23 ± 1 °C with a Kimble Glass specific gravity pycnometer (Vineland, NJ).

2.8. Refractive Index. Refractive index measurements were conducted at 23 ± 1 °C using a Bausch & Lomb Abbe-3L refractometer.

2.9. Viscosity. Kinematic viscosities were determined at 30 ± 1 °C using a Cannon-Manning semi-micro capillary viscometer (State College, PA).

2.10. Thermal Stability Analysis. Thermogravimetric analysis (TGA) was done using a TGA 2050 instrument (TA Instruments Inc., Thermal Analysis & Rheology, New Castle, DE). Samples (ca. 20 mg) were placed on the platinum pans and heated at 10 °C min^{-1} from room temperature to 600 °C under a dynamic nitrogen atmosphere. The decomposition temperatures were reported as the temperatures of 1%, 5%, and 50% weight loss of the sample.

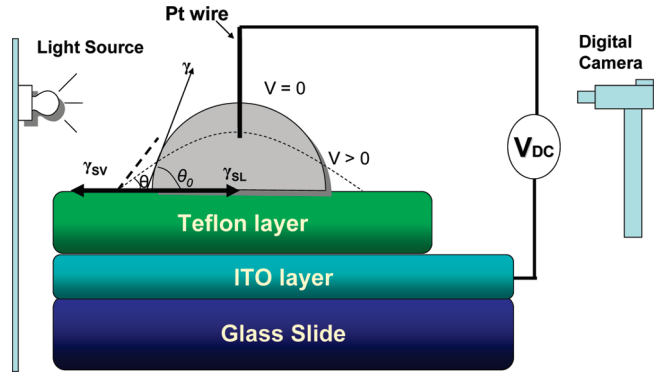

FIGURE 3. Electrowetting experimental setup. Here, γ, γ_{SV}, and γ_{SL} are the interfacial tensions associated with the liquid/vapor, solid/vapor, and solid/liquid interfaces.

2.11. Electrowetting Experiments. Electrowetting experiments were conducted by using a slightly modified contact angle goniometer (www.ksvltd.com, Monroe, CT). Figure 3 shows the arrangement for the electrowetting experiment. Indium tin oxide (ITO, 30 nm thickness) precoated unpolished float glass slides (www.delta-technologies.com, Stillwater, MN) were used as purchased. They were dip-coated in a 4% (w/v) Teflon AF1600 (www2.dupont.com, Wilmington, DE) in Fluoroinert FC75 solvent (www.fishersci.com, Barrington, IL) solution. The dipping speed was approximately 0.78 ± 0.03 mm s^{-1} in a custom-made dipcoater. Only three-fourths of the slide was dipped in the solution; then the movement was stopped for 5 s, and after that the slide was raised at the same speed. The coated slides were kept in an oven at 112 °C for 6 min, at 165 °C for 5 min, and at 328 °C for 15 min. Once Teflon-coated glass slides were taken out from the oven, they were allowed to reach room temperature. Then they were washed thoroughly with acetone and deionized water followed by air drying. A capillary tube was used to place a drop of IL on top of the Teflon layer. CAM 200 software (www.ksvltd.com, Monroe, CT) was used to calculate the drop volume; it was between 5 ± 2 μL for all experiments. A Keithley 2400 SourceMeter (www.keithley.com, Cleveland, OH) was used to apply voltage in 5 V increments from 0 to +70 V. The positive probe was connected to the Pt wire, and the negative probe was connected to the ITO layer (see Figure 3). Afterward, the above procedure was repeated for 0 to −70 V for a fresh drop of IL placed at a different position on the surface. At each voltage increment a picture was taken and then CAM 200 software was used to measure corresponding contact angles. Finally, the contact angle versus voltage curves were plotted.

All tested ILs were kept in a vacuum oven at room temperature overnight with phosphorus pentoxide (P_2O_5) to minimize the water content.

3. RESULTS AND DISCUSSION

The synthetic strategy involved in these linear tricationic ILs was different from previously reported ionic liquids for the following reasons. (1) Core 1 (Scheme 1) was designed and synthesized in-house. It was separated and isolated from the dicationic and polycationic impurities that were formed during the reaction, by running through a flash chromatography column (SiO_2 60 Å, CH_2Cl_2/CH_3OH 1:9). (2) In previous dicationic and trigonal tricationic IL syntheses, isopropyl alcohol was used as the reaction solvent in most cases (9). However, when alcohols were used, the basic imidazole tended to deprotonate the alcohol, enabling unwanted nucleophilic substitution reactions (11). This complicated the separation of the pure LTILs from the reaction mixture.

Table 1. Physiochemical Properties of Linear Tricationic Ionic Liquids

						thermal stability[d]			miscibility[e,f]	
ionic liquid	mol wt	mp[a] (°C)	density[b] (g cm^{-3})	refractive index	viscosity[c] (cSt)	99% w	95% w	50% w	heptane	water
2a-NTf_2	1352.25	−53.58	1.65	1.45	1800	334	400	444	I	I
2b-NTf_2	1435.29	−53.17	1.54	1.44	2400	350	390	430	I	I
2c-NTf_2	1504.44	−36.61	1.36	1.48	4200	320	390	450	I	I
2d-NTf_2	1507.37	−41.58	1.46	1.45	2100	360	410	440	I	I
2b-BF_4[f]	856.55	−18.32	1.33			191	308	369	I	M
2b-TfO[f]	1043.18	−42.63	1.28			290	376	430	I	M
3a-NTf_2	1240.03	−57.85	1.57	1.44	372	320	380	480	I	I
3b-NTf_2	1324.19	−51.54	1.41	1.49	429	330	380	470	I	I
3c-NTf_2	1391.14	−36.83	1.43	1.47	840	340	370	470	I	I
3d-NTf_2	1396.30	−45.41	1.38	1.45	770	355	400	440	I	I
4a-NTf_2	1155.88	−24.54	1.54	1.46	1200	290	360	410	I	I
4b-NTf_2	1240.04	−44.13	1.48	1.49	600	310	370	470	I	I
4c-NTf_2	1308.07	−27.26	1.41	1.48	4080	300	350	470	I	I
4d-NTf_2	1312.14	71−72	1.59			320	390	480	I	I

[a] Determined by using a differential scanning calorimeter upon heating cycle; melting points are reported as the onset temperature of the melting endotherm. [b] Determined by using a pycnometer,. [c] Measured using a capillary viscometer at 30 °C. [d] The decomposition temperature was determined by using TGA: 99% w, temperature at 1% mass decrease of sample; 95% w, temperature at 5% mass decrease of the sample; 50% w, temperature at 50% mass decrease of sample. [e] Legend: I, immiscible; M, miscible. [f] Amorphous solid.

Therefore, the solvent used in the synthesis of Core 1 was dimethylformamide (DMF). This was because DMF dissolved sodium imidazole (NaIM) and it minimized the side reactions that take place with protic solvents. Other reaction solvents for the synthesis of ILs involving imidazolium moieties were found to be acetonitrile (ACN) and tetrahydrofuran (THF). However, isopropyl alcohol can be used as the solvent in reactions involving tripropylphosphonium, which has a weakly basic character compared to imidazole.

In this study, 14 linear tricationic ionic liquids were synthesized and their physicochemical properties were investigated. The results are given in Table 1.

Phase transition temperatures, including glass transition temperatures (T_g) (see Figures S21−S23 in the Supporting Information), were determined using differential scanning calorimetry (DSC). LTILs show significantly lower glass transition temperatures (except for **4d**) compared to many other types of ILs in the literature, such as symmetrical dicationic ILs (9). It has been shown for most dicationic ILs that when the chain length is smaller than three methylene units, the IL becomes solid regardless of other structural changes (9c). However, we found that LTILs with C3 linkage chains (**4a**−**c**) (Figure 1) do exist as RTILs when the counteranion is bis(trifluoromethylsulfonyl)imide (NTf_2^-). This can be explained by the relative flexibility of the LTILs. Unlike trigonal tricationic ILs, the LTILs have greater conformational degrees of freedom which help to minimize charge repulsion interactions (14). The T_g values are mainly governed by the size and charge distribution of the anion and/or cation (15). According to the literature, most ILs containing NTf_2^- are observed to be liquids at room temperature (9, 15, 17). When the negative charge carrying moiety is a halide, X^- ($X^- = F^-$, Cl^-, Br^-, I^-), BF_4^-, TfO^- (trifluoromethanesulfonate), or PF_6^-, the ILs tend to have higher melting points (9).

The LTILs with methylimidazolium charge carrying moieties **2a**−**4a** showed the lowest melting temperatures of the series. According to the melting point data in Table 1, the butylimidazole cationic moiety produces ILs with higher melting points compared to the methylimidazole moiety. This is probably because of the butyl group's greater van der Waals interactions. Relatively higher melting temperatures were observed when the IL incorporated the benzylimidazole moiety, mainly because of the additional $\pi-\pi$ stacking introduced by the phenyl groups (9).

The kinematic viscosities of these LTILs range from 372 to 4200 cSt at 303 K. LTILs with the C6 linkage chain generally showed lower viscosities ranging from 60−840 cSt. Typically, monocationic ILs have lower kinematic viscosities (16). The viscosities are markedly higher in ILs with benzyl groups (see Table 1). The same phenomenon was observed in dicationic and trigonal tricationic ILs (9). It is interesting to note that ILs with a C3 linkage chain have higher viscosities compared to ILs with C6 linkage chains and lower viscosities when compared to those with C10 linkage chains. According to these results, ILs having C3 linkage chains seem to possess greater ionic nature, owing to the closeness of the charged groups. When the distance between charged groups is increased to six methylene units (∼8.9 Å), as in ILs with C6 linkage chains, the ionic nature is reduced, resulting in lower viscosity. However, when the linkage chain is further increased up to 10 methylene units (∼14 Å), higher viscosities are observed, again due to the increase of intermolecular van der Waals interactions over ionic interactions (15).

The densities of LTILs with accompanying NTf_2^- anions range from 1.36 to 1.65 g cm^{-3}. The lowest density was observed for **2c**, which has a benzylimidazolium cation and C10 linkage chains. Higher density values are obtained for LTILs with methylimidazolium groups. Moreover, when the chain length of the substituent at the 3-position of the

Table 2. Electrowetting Properties of Linear Tricationic Ionic Liquids[a]

ionic liquid	θ_0	$\Delta\theta_L$	$\Delta\theta_R$	V_L	V_R
2a	83	16	18	−40	50
2b	80	14	15	−35	30
2c	83	17	18	−50	40
2d	80	16	16	−60	40
3a	85	13	18	−40	40
3b	81	15	14	−30	35
3c	84	12	16	−35	40
3d	78	11	11	−30	35
4a	82	21	16	−35	40
4b	88	19	14	−40	50
4c	86	23	16	−60	55
4d					
IL13[b]	77	>25	>20	<−70	>70
IL14[b]	88	18	18	−65	60
IL15[b]	77	20	25	−55	60
IL16[b]	82	>15	>14	<−70	>70

[a] Legend: θ_0, contact angle at zero voltage; $\Delta\theta_L$, apparent contact angle change at negative voltages; $\Delta\theta_R$, apparent contact angle change at positive voltages; V_L, saturation voltage in the negative voltage realm; V_R, analogous saturation voltage in the positive voltage realm. [b] Data taken from ref 8a.

imidazole increases from methylimidazolium to butylimidazolium, the density decreases (**2a**,**b**, **3a**,**b**, and **4a**,**b**). Similar observations have been reported for monocationic and dicationic ILs as well (9).

The refractive indices of the LTILs range from 1.44 to 1.49 and lie within the general range observed for monocationic ILs (17). The solubility of these LTILs parallels that of monocationic ILs (13, 17), in which all Br^-, BF_4^-, and TfO^- (trifluoromethanesulfonate) salts synthesized were soluble in water, while all NTf_2^- salts were insoluble in water. All of the LTILs synthesized were insoluble in *n*-heptane.

For RTILs to be used in applications such as high-temperature organic reactions (12) and as GC stationary phases, they should possess a good thermal stability. Generally, phosphonium cation based ILs show higher thermal stabilities compared to nitrogen cation based ILs such as imidazolium and pyrolidinium ILs (9, 13). This trend was clearly seen in this study as well. LTIL **2d**, with two tripropylphosphonium cations, has the highest thermal stability, displaying only 5% thermal degradation at 410 °C.

The electrowetting properties of ILs are given in Table 2. Figure 4 shows the electrowetting curves of linear tricationic ionic liquids with C6 linkage chains, and Figure 6 shows the electrowetting curves of benzylimidazolium-substituted tricationic ionic liquids with different linkage chain lengths and core structures.

θ_0 Values. Since there is no external voltage at θ_0, only the three interfacial tensions (solid/liquid, liquid/air, and air/solid) govern the θ_0 value. However, solid (Teflon) is common in all experiments; therefore, only the surface tension of the IL governs the θ_0 value (8a). The higher the surface tension value of the IL, the higher the θ_0 value obtained (8a). Therefore, from the observed θ_0 values the relative surface tension of these ILs can be deduced. This is a good indirect

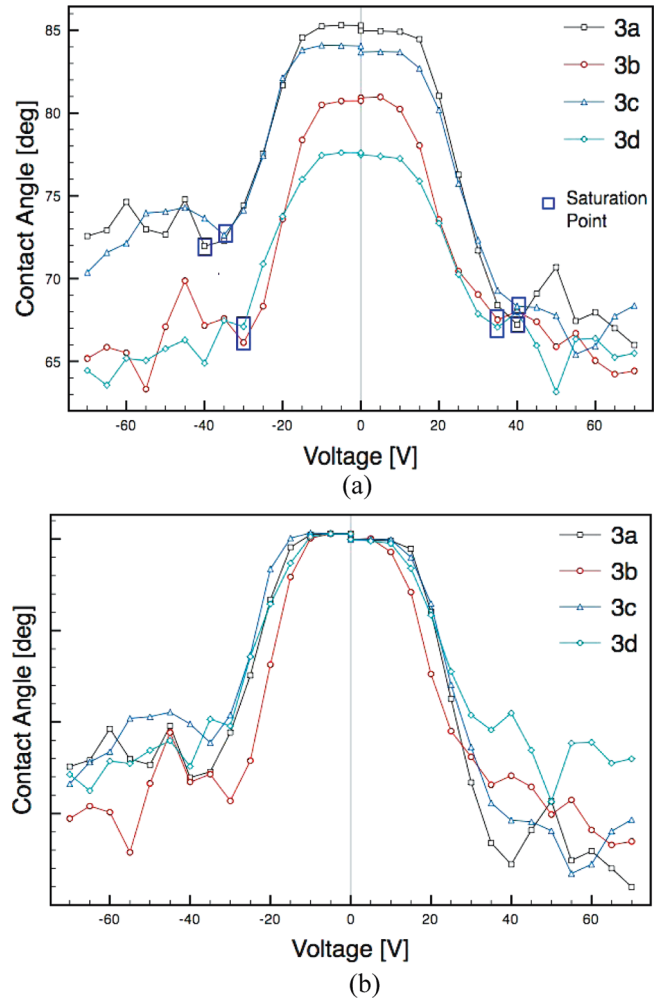

FIGURE 4. Electrowetting curves of (a) linear tricationic ionic liquids with C6 linkage chains and (b) linear tricationic ionic liquids with C6 linkage chains overlaid normal to the maximum θ_0 value.

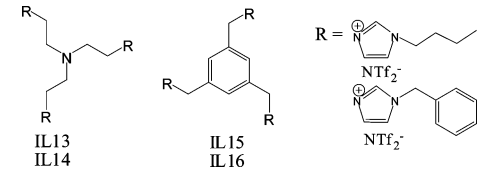

FIGURE 5. Structures of rigid core tricationic ionic liquids.

method to evaluate the relative surface tensions of this new class of ILs. According to Figure 4 and Table 2, for ionic liquids **3a**−**d**, which have the same anion (NTf_2^-) and the same linkage chain length (C6), the θ_0 values decrease in the order **3a** > **3c** > **3b** > **3d**. This decrease is solely due to the end cationic moieties. The θ_0 value directly correlates with the surface tension. Therefore, the surface tension of these ILs decrease on the basis of the cation in the order methylimidazolium > benzylimidazolium > butylimidazolium > tripropylphosphonium.

According to Figure 6 and Table 2, by considering θ_0, surface tension values of benzyl-substituted ILs decrease in the order **IL 14** > **4c** > **3c** > **2c** > **IL 16**. Surface tension values of liquids tend to increase with an increase in hydrophilicity (27). **IL 14**, with a nitrogen core (see Figure 5), has more hydrophilic character compared to **IL 16**, with a mesitylene

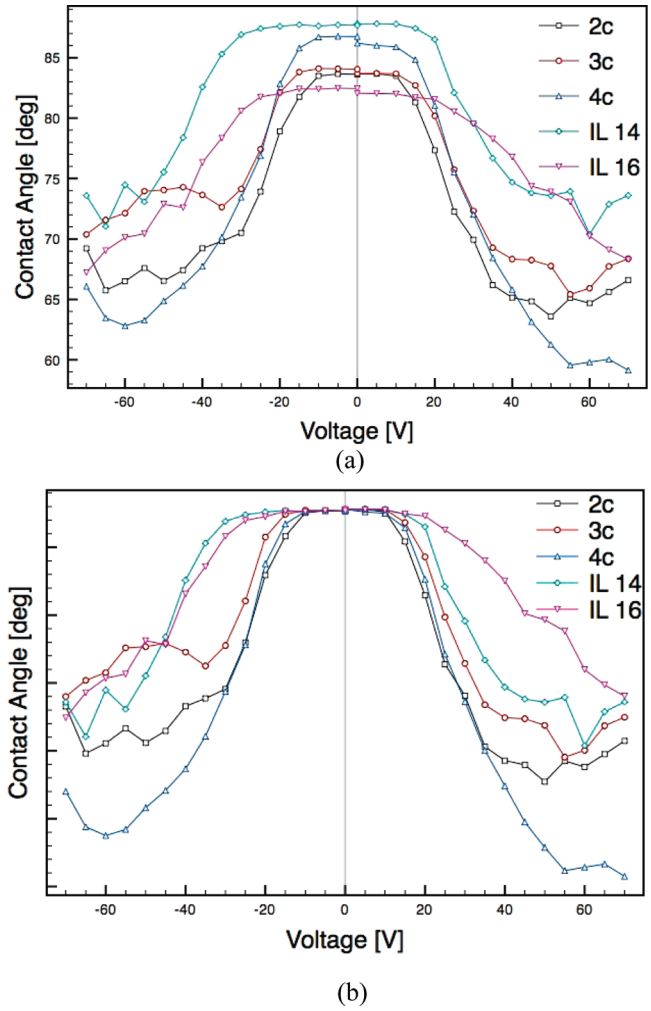

FIGURE 6. Electrowetting curves of (a) benzylimidazole-substituted linear and rigid type tricationic ionic liquids and (b) benzylimidazole-substituted linear and rigid type tricationic ionic liquids overlaid normal to the maximum θ_0 value.

core. Therefore, **IL 14** has higher surface tension than **IL 16**, which is reflected by the θ_0 value. Similarly, when the alkyl chain length of the LTILs increases from C3 to C10 as in **4c** to **2c**, the hydrophobic character increases and therefore surface tension decreases.

Rigid Core structure vs Flexible Core Structure. Figure 6a shows the electrowetting curves of benzylimidazole-substituted ILs, both rigid core (**IL 14**, **IL 16**) and flexible core (**2c**−**4c**) ILs. In Figure 6b curves are overlaid normal to the maximum θ_0 value. According to Figure 6b and Table 2, it can be clearly observed that rigid core ILs (**IL 14** and **IL 16**) have V_L and V_R values wider than those of flexible core ILs (**2c**−**4c**). However, flexible core ILs produced much smoother curves than rigid core ILs. This means that their electrowetting properties are much closer to the ideal behavior expected according to Young's and Lippmann's equations. Similar observations can be seen in butylimidazolium -substituted rigid ILs (**IL 13**, **IL 15**) and flexible ILs (**2b**−**4b**) as well (see Figure S19 in the Supporting Information).

Effect of End Groups. Electrowetting curves of linear tricationic ILs with C6 linkage chains, each with four different end groups, are plotted in Figure 4a. In Figure 4b these curves are overlaid normal to the maximum θ_0 value. There are no significant differences in electrowetting properties by changing the end groups, except for θ_0 values. θ_0 values are different from one IL to another, due to surface tension differences, which was explained previously. It is interesting to note that the electrowetting properties of these ILs are fairly similar, regardless of their different physicochemical properties. This unique situation enables one to choose an ionic liquid with the desired physical property from a large library of ionic liquids that have the same electrowetting properties. For example, if fast changes in contact angles are required in an electrowetting application, ILs with lower viscosities can be used. LTIL **3a** has significantly lower viscosity than **3c**, but their electrowetting properties are approximately the same (Table 2). These observations are valid for the other C3 linkage chain and C10 linkage chain ILs as well (see Figures S16 and S17 in the Supporting Information).

Examining electrowetting properties and physical properties of the relevant ILs listed here, one can find a suitable replacement for aqueous electrowetting in traditional EWOD-based devices.

CONCLUSION

The synthesis and physiochemical properties of 14 linear tricationic ionic liquids were reported, and these have been explored as potential electrowetting liquids. These LTILs have shown high thermal stabilities and considerably high viscosities compared to traditional monocationic and dicationic ionic liquids. Most of the LTILs synthesized were room-temperature ILs due to their higher structural flexibilities. This structural flexibility was advantageous in electrowetting applications, as LTILs were observed to be much closer to the ideal behavior described in Young's and Lippmann's equation than any other ionic liquids reported in the literature.

Acknowledgment. We thank the Robert A. Welch Foundation (Grant No. Y-0026) for funding this project.

Supporting Information Available: Text and figures giving general methods, NMR spectra of the synthesized ionic liquids, electrowetting curves, and selected DSC thermograms. This material is available free of charge via the Internet at http://pubs.acs.org.

REFERENCES AND NOTES

(1) Welton, T. *Chem. Rev.* **1999**, *99*, 2071–2083.
(2) Rogers, R. D.; Seddon, K. R. *ACS Symp. Ser.* **2003**, *No. 856*, 2–70.
(3) Plechkova, N. V.; Seddon, K. R. *Chem. Soc. Rev.* **2008**, *37*, 123–150.
(4) Rogers, R. D.; Seddon, K. R. *Science* **2003**, *302*, 792–793.
(5) (a) Soukup-Hein, R. J.; Remsburg, J. W.; Dasgupta, P. K.; Armstrong, D. W. *Anal. Chem.* **2007**, *79*, 7346–7352. (b) Soukup-Hein, R. J.; Remsburg, J. W.; Breitbach, Z. S.; Sharma, P. S.; Payagala, T.; Wanigasekara, E.; Huang, J.; Armstrong, D. W. *Anal. Chem.* **2008**, *80*, 2612–2616.
(6) (a) Anderson, J. L.; Armstrong, D. W.; Wei, G. *Anal. Chem.* **2006**, *78*, 2892–2902. (b) Ding, J.; Armstrong, D. W. *Chirality* **2005**, *17*, 281–292. (c) Anderson, J. L.; Ding, R.; Ellern, A.; Armstrong, D. W. *J. Am. Chem. Soc.* **2005**, *127*, 593–604. (d) Payagala, T.;

Zhang, Y.; Wanigasekara, E.; Huang, K.; Breitbach, Z. S.; Sharma, P. S.; Sidisky, L. M.; Armstrong, D. W. *Anal. Chem.* **2008**, *81*, 160–173.
(7) Vaher, M.; Koel, M.; Kaljurand, M. *J. Chromatogr. A* **2002**, *979*, 27–32, and references therein.
(8) (a) Nanayakkara, Y. S.; Moon, H.; Payagala, T.; Wijeratne, A. B.; Crank, J. A.; Sharma, P. S.; Armstrong, D. W. *Anal. Chem.* **2008**, *80*, 7690–7698. (b) Millefiorini, S.; Tkaczyk, A. H.; Sedev, R.; Efthimiadis, J.; Ralston, J. *J. Am. Chem. Soc.* **2006**, *128*, 3098–3101. (c) Law, G.; Watson, P. R. *Langmuir* **2001**, *17*, 6138–6141.
(9) (a) Payagala, T.; Huang, J.; Breitbach, Z. S.; Sharma, P. S.; Armstrong, D. W. *Chem. Mater.* **2007**, *19*, 5848–5850. (b) Sharma, P. S.; Payagala, T.; Wanigasekara, E.; Wijeratne, A. B.; Huang, J.; Armstrong, D. W. *Chem. Mater.* **2008**, *20*, 4182–4184. (c) Anderson, J. L.; Ding, R.; Ellern, A.; Armstrong, D. W. *J. Am. Chem. Soc.* **2005**, *127*, 593–604.
(10) (a) Wasserscheid, P., Welton, T., Eds. *Ionic Liquids in Synthesis*; Wiley-VCH: Weinheim, Germany, 2003. (b) Bonhote, P.; Dias, A.-P.; Papageorgiou, N.; Kalyanasundaram, K.; Graetzel, M. *Inorg. Chem.* **1996**, *35*, 1168–1178.
(11) Catalan, J.; Claramunt, R. M.; Elguero, J.; Laynez, J.; Menendez, M.; Anvia, F.; Quian, J. H.; Taagepera, M.; Taft, R. W. *J. Am. Chem. Soc.* **1988**, *110*, 4105–4111.
(12) (a) Han, X.; Armstrong, D. W. *Org. Lett.* **2005**, *7*, 4205–4208. (b) Gordon, C. M. *Appl. Catal. A: Gen.* **2001**, *222*, 101–117.
(13) Bradaric, C. J.; Downard, A.; Kennedy, C.; Robertson, A. J.; Zhou, Y. *Green Chem.* **2003**, *5*, 143–152.
(14) (a) Abramowitz, R.; Yalkowsky, S. H. *Pharm. Res.* **1990**, *7*, 942–947. (b) Dearden, J. C. *Sci. Total Environ.* **1991**, *59*, 109–110.
(15) Zhou, Z.-B.; Matsumoto, H.; Tatsumi, K. *ChemPhysChem* **2005**, *6*, 1324–1332.
(16) (a) Wasserscheid, P., Welton, T., Eds. *Ionic Liquids in Synthesis*; Wiley-VCH: Weinheim, Germany, 2003. (b) Bonhote, P.; Dias, A.-P.; Papageorgiou, N.; Kalyanasundaram, K.; Graetzel, M. *Inorg. Chem.* **1996**, *35*, 1168–1178.
(17) (a) Sheldon, R. *Chem. Commun.* **2001**, 2399–2407. (b) Visser, A. E.; Swatloski, R. P.; Rogers, R. D. *Green Chem.* **2000**, *2*, 1–4. (c) Keim, W.; Wasserscheid, P. *Angew. Chem., Int. Ed.* **2000**, *39*, 3772–3789.
(18) Moon, H.; Wheeler, A. R.; Garrell, R. L.; Loo, J. A.; Kim, C. *Lab Chip* **2006**, *6*, 1213–1219.
(19) Pollack, M. G.; Fair, R. B.; Shenderov, A. D. *Appl. Phys. Lett.* **2000**, *77*, 1725–1726.
(20) Wheeler, A. R.; Moon, H.; Kim, C.; Loo, J. A.; Garrell, R. L. *Anal. Chem.* **2004**, *76*, 4833–4838.
(21) Berge, B.; Peseux, J. *Eur. Phys. J. E: Soft Matter* **2000**, *3*, 159–163.
(22) Hayes, R. A.; Feenstra, B. J. *Nature* **2003**, *425*, 383–385.
(23) (a) Dubois, P.; Marchand, G.; Fouillet, Y.; Berthier, J.; Douki, T.; Hassine, F.; Gmouh, S.; Vaultier, M. *Anal. Chem.* **2006**, *78*, 4909–4917. (b) Millefiorini, S.; Tkaczyk, A. H.; Sedev, R.; Efthimiadis, J.; Ralston, J. *J. Am. Chem. Soc.* **2006**, *128*, 3098–3101.
(24) Dubois, P.; Marchand, G.; Fouillet, Y.; Berthier, J.; Douki, T.; Hassine, F.; Gmouh, S.; Vaultier, M. *Anal. Chem.* **2006**, *78*, 4909–4917.
(25) Chatterjee, D.; Hetayothin, B.; Wheeler, A. R.; King, D. J.; Garrell, R. L. *Lab Chip* **2006**, *6*, 199–206.
(26) (a) Moon, H.; Bindiganavale, S.; Nanayakkara, Y. S.; Armstrong, D. W. Proceedings of the Seventh International ASME Conference on Nanochannels, Microchannels and Minichannels ICNMM2009; Pohang, South Korea, June 22—24, 2009. (b) Kunchala, P.; Moon, H.; Nanayakkara, Y. S.; Armstrong, D. W. Proceedings of the ASME 2009 Summer Bioengineering Conference (SBC2009) ; Lake Tahoe, CA, June 17—21, 2009.
(27) Zhu, Y.-P.; Rosen, M. J.; Morrall, S. W. *J. Surfactants Deterg.* **1998**, *1* (1), 1–9.

AM900519J